Application of phase diagrams in the curing of unsaturated polyester resins with low-profile additives

Laurent Suspène, Dominique Fourquier and Yeong-Show Yang
CRAY VALLEY-TOTAL Group, Research Center of Verneuil, BP 22, 60550 Verneuil en Halatte, France
(Received 18 December 1989; revised 29 June 1990; accepted 3 July 1990)

A cloud point curve (CPC) type phase diagram had been established for the system of styrene–unsaturated polyester resin with or without low profile additive (LPA) before curing. The final morphology of the cured system was correlated to the CPC phase diagram. Changing the molecular characteristics or molecular weight distribution of the unsaturated polyester (UP) prepolymer and/or LPA might greatly influence the prepolymer's miscibility with styrene and the ternary phase diagram of styrene–UP prepolymer–LPA systems, and finally change the curing morphology. Adding the LPA in a styrene–UP prepolymer mixture might cause phase separation accompanied by a fractionation effect which excludes high molecular weight polymer from the styrene and LPA-rich phase. The fractionated phase separation phenomenon was observed by light scattering and microscopic measurements. Differential scanning calorimetry measurements showed that the formation of phase separation seemed to be parallel to the curing conversion and microvoids were found around and after the point of the maximum reaction rate. Transmission electron micrographs clearly showed that the microvoids compensating the resin shrinkage were formed in the low-profile phase. The solvent extract analysis showed that the soluble phase of the cured resin included residual styrene, LPA, uncrosslinked polystyrene and some saturated polyester molecules. A novel low profile mechanism is proposed based on the concepts of phase diagrams and fractionated phase separation.

(Keywords: low-profile additive; unsaturated polyester resin; phase diagram; phase separation; cloud point curve)

INTRODUCTION

Unsaturated polyester (UP) resin is one of the most important thermoset resins for composite applications. It is particularly used in sheet moulding compounds (SMC) for manufacturing automotive parts. Many researchers[1–9] have studied the curing kinetics of the bulk copolymerization of styrene–UP resins. The rheological characterization and measurements during curing have also been carried out[10–12]. Although insight into the reaction mechanism and the processing characteristics of SMC compounds have been obtained, there has only been limited effort to apply this knowledge to understand the low profile effect which can compensate for polymerization shrinkage of the resin[13]. The high polymerization shrinkage of the UP resin may cause several moulding problems such as poor surface quality, warpage, sink marks, internal cracks, blisters and dimension control[14,15].

During curing, the resin tends to shrink away from the mould walls due to polymerization shrinkage. The shrinkage force creates internal stresses which lead to surface and structural flaws. The former cause surface problems and the latter lead to the mould sink mark and dimension problems. In order to eliminate most of the problems mentioned, low profile additives (LPA) such as poly(methyl methacrylate) (PMMA) and poly(vinyl acetate) (PVAc) are widely used in the curing of UP resins to compensate for the resin shrinkage. Numerous investigations have been carried out[13–25] to explain the mechanism of low profile behaviour. Although the mechanism is not fully understood, the shrinkage compensation is mostly believed to be due to the formation of microvoids in the interfacial region between the resin and additive phase[16,17,22–24]. This indicates that a phase separation during the curing process is an important parameter because it provides a two-phase system to allow the formation of microvoids for the shrinkage compensation.

Phase separation is caused by a change in miscibility of the monomer, prepolymer and additives during curing[18]. The miscibility of the system can be expressed by a phase diagram. Recently, Suspène and Pascault[26,27] studied phase diagrams and interfacial properties of styrene–UP prepolymer–elastomer additive systems and explained the cured morphologies by phase diagrams. The added elastomer additives were used to improve the resin impact strength and had no volume compensation effect. The correlation of a system phase diagram and cured morphology can be easily applied for the low profile resin systems. This paper studies the phase separation phenomena on curing UP resins by their phase diagrams and attempts to explain the low profile mechanism for the process.

EXPERIMENTAL

Materials

Two SMC grade polyester resins (65 wt% in styrene solution) containing M1 and M2 UP prepolymers were used. Both M1 and M2 prepolymers are 1:1 mixtures of maleic anhydride and propylene glycol. They have similar number average molecular weights with about 10

0032-3861/91/091593-12

Table 1 Molecular characteristics of M1 and M2 UP prepolymers

Prepolymer	M_n[a]	M_w/M_n[a]	I_A[b]	I_{OH}[b]
M1	1689	7.48	30	50
M2	1480	3.14	20	60

[a] M_n, M_w measured by a differential refractometer detector
[b] I_A, I_{OH} in mg KOH per g resin: acid and hydroxyl indices

vinylene groups per molecule. However, the M1 prepolymer had a broader molecular weight distribution (*MWD*) than the M2 prepolymer. Moreover, M1 showed a higher acid index and lower hydroxyl index. Their molecular characteristics are given in *Table 1*.

The investigated low profile additives were PVAc (LP 40A, Union Carbide, $M_n = 40\,000$ g mol^{-1}, 40 wt% styrene solution) and four polyurethanes (PU2500, PU9000, PU11000 and PU20000) with molecular weights from 2500 to 20 000 g mol^{-1}. The composition of the resins and the LPAs was adjusted as required. For polymerization studies, a composition of 45.4 wt% styrene, 41.3 wt% UP prepolymer and 13.3 wt% LPA was chosen and 1.5% t-butyl perbenzoate was used as a high temperature initiator.

Instrumentation and measurements

Cloud point and phase diagrams. A liquid mixture could be transparent or opaque (cloudy) depending on composition and temperature. Theoretically, if the refractive indices of the mixing components are sufficiently different, a transparent mixture represents a miscible one-phase system and a cloudy mixture represents an immiscible two-phase system. A cloud point is the point at which the system changes its transparency from transparent to cloudy or changes its opacity from cloudy to transparent due to change in composition or temperature.

In this study, the cloud points of styrene–UP resins, with or without LPA, were obtained by observing the change of transparency of the system by adding styrene monomer in the mixture at constant temperature (i.e. isothermal cloud point) or by increasing the temperature of a constant composition mixture (i.e. non-isothermal cloud point). The measurements were taken under moderate agitation.

Chromatography. The styrene content of a resin mixture was determined by gas chromatography (g.c., Hewlett Packard 3380A, with Intersmat IGC121). Gel permeation chromatography (g.p.c., Perkin Elmer, series 10) was used to measure the polymer molecular weight at room temperature with the following column combinations: 50, 100, 500, 1000 Å and a mix column with average size of 500 Å. The dual detector system consisted of an ultraviolet (u.v.) detector and a differential refractometer (RI) in sequence in the flow direction. The RI was used to measure the molecular weights of all the species in the systems. The u.v. detector used a monochromatic light at 254 nm (for vinylene groups) to measure the molecular weight of UP resin without interference from PVAc. All the g.p.c. curves were analysed by using the calibration curve obtained with standard samples of monodispersed polystyrene to estimate the molecular weight.

Calorimetry. The reaction kinetics of the resins were measured by a differential scanning calorimeter (Perkin-Elmer, DSC2). A well-mixed sample of 10–20 mg was transferred to a volatile aluminium sample pan capable of withstanding 2×10^5 Pa internal pressure after sealing. The reaction was carried out in the scanning mode from 30 to 250°C at a heating rate of 5°C min^{-1} with an empty pan as reference. The total heat of reaction was determined from the area under the scanning curve. The reaction conversion was calculated by the ratio of integrated heat to the total reaction heat. For the measurement of the glass transition temperature, the differential scanning calorimetry scans (d.s.c.) were recorded at 20°C min^{-1}, with a signal output of 1 mV.

Phase separation. A self-made low angle laser light scattering (LALLS) apparatus was introduced to follow the phase separation during the curing of UP resins. The detecting angle was fixed at 10–20° for measuring microdomains >100 nm. For a miscible system, the measurement of light scattering would be theoretically zero. The measured light scattering intensity would be a function of the concentration of microdomains.

A thin layer of UP resin bounded by two cover glasses was inserted into a microscope hot-stage (Mettler, FP-80). The phase separation during the reaction was followed by measuring the scattered light intensity from 30 to 250°C with a heating rate of 5°C min^{-1}. At a certain time, the reaction was stopped by quenching the sample into liquid nitrogen. The micrograph of the quenched sample was taken under an optical microscope at room temperature.

Morphology. For morphological studies, the resins were moulded at 150°C at a pressure of 70×10^5 Pa for 4 min. A 4 mm thick Teflon ring was employed as the spacer. The moulded samples were broken into several pieces. One piece was etched in acetone for 30 min to dissolve the soluble material on the fracture surface. This piece was then gold-coated and the fracture was viewed by a scanning electron microscope (Cambridge stereoscan 600). In addition, another piece was microtomed and then stained by $RhCl_4$ for transmission electron microscope (Philips, EH31) observation.

Extract analysis. One piece of moulded sample was ground into powder and then extracted by dichloromethane (DCM) for 24 h. The composition of the extract was analysed by ^{1}H nuclear magnetic resonance (n.m.r., Bruker 1M360) and by g.p.c..

RESULTS

Phase diagrams

Figure 1 shows a typical triangle diagram of a ternary system of styrene–UP–LPA. The UP represents M1 (or M2) prepolymer and PVAc is used as the LPA. The open square symbols show isothermal cloud points of the ternary system of styrene–M1–PVAc measured at 23°C. An isothermal ternary cloud point curve (CPC) could be obtained by connecting all the isothermal cloud points to form an envelope. Inside the envelope is a two-phase region in which the system is cloudy after mixing and will undergo phase sedimentation after storage. Outside the envelope is a one-phase region in which all the mixtures are miscible and transparent at the specific

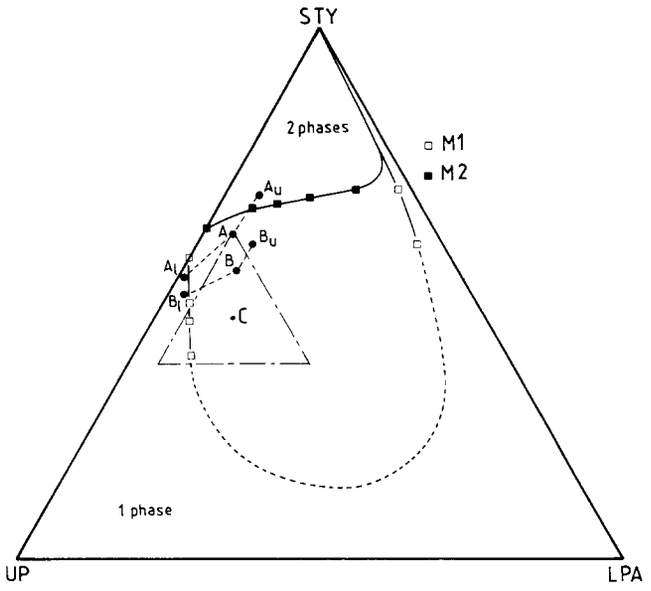

Figure 1 Phase diagram of styrene–M1 prepolymer–PVAc ternary systems. □, Experimental cloud point of styrene–M1–PVAc at 23°C; ■, experimental cloud point of styrene–M2–PVAc at 23°C; solid lines and broken lines, isothermal CPC at 23°C; dashed triangle, range of industrial formulation for low profile UP resin; A and B, studied compositions; subscripts u and l, upper and lower phases, respectively; C, composition chosen for moulding studies

temperature. If the mixture contains enough UP and/or LPA it is highly viscous and it is difficult to observe the corresponding cloud point. For that reason, the isothermal CPC is not experimentally completed, so that the bottom part is experimentally shown as a broken line instead of a solid line. However, it is reasonable that the bottom part of the envelope does not reach the UP–LPA line because the UP prepolymer is always miscible with PVAc. For the system of styrene and M1 prepolymer a cloud point exists at 23°C. This means that the M1 prepolymer is only partially miscible with styrene[28,29].

The dashed triangle represents the formulation range of typical industrial UP resins. For M1 prepolymer most of the formulations are not miscible and will separate into two phases after a period of storage. For example, point A represents a formulation of 5 wt% PVAc, 33 wt% M1 and 62 wt% styrene. The mixture is cloudy after mixing and becomes two phases in a test tube on storing for 2 days at room temperature. The upper phase is ~60% of the total volume. The compositions of the upper and the lower phases are determined by g.c. (for styrene content) and by acid titration (for UP content). The LPA content is calculated with the measured styrene and UP contents. The upper phase is shown as point A_u in *Figure 1*; the lower phase is shown as point A_l. Similarly, the formulation B (9 wt% PVAc, 36 wt% M1 and 55 wt% styrene) also forms two phases shown as points B_u (upper phase) and B_l (lower phase). That the points A, A_u and A_l (or B, B_u and B_l) are not on a straight tie line is due to data manipulating deviation[26]. For both formulations, the upper phases are rich in styrene monomer and PVAc, while the lower phases are rich in M1 prepolymer.

Figure 2 shows g.p.c. (*MWD*) curves of the prepolymers and the LPA contained in phases A_u and A_l. The g.p.c. curves of the M1 prepolymer are also shown in the figure for comparison. Their g.p.c.–RI curves are shown in *Figure 2a*. The styrene peaks are not shown. *Figure 2a* clearly shows that A_u contains PVAc, while A_l has an insignificant amount of PVAc. This confirms the results of the composition analysis. *Figure 2b* shows the g.p.c.–u.v. curves of the A_u and A_l phases. Because they are measured with a u.v. detector at 254 nm, the interference of PVAc has been eliminated. The styrene peaks are not shown. All the curves represent the *MWD* of the UP prepolymer only. It is clearly shown that all the three *MWD* curves are not identical. The measured molecular weights of UP prepolymers in A, A_u and A_l are shown in *Table 2*. One can conclude that the polydispersities of the UP prepolymers remaining in the upper and lower phases are not the same and are different from that of the original M1 prepolymer. It is also observed that phase A_l contains more high molecular weight prepolymer (short elution time, $M_w = 34\,277$ g mol^{-1}) than phase A_u ($M_w = 5693$ g mol^{-1}). In other words, the high molecular weight prepolymer is fractionated by the PVAc and probably remains in the lower resin-rich phase.

Theoretically, a phase diagram should be drawn by the phase points such as A_u, B_u, A_l and B_l and it should be identical with the isothermal CPC. Koningsveld and Staverman[30] revealed that the phase separation in a polydispersed polymer solution would be accompanied by a fractionation phenomenon that causes a change of

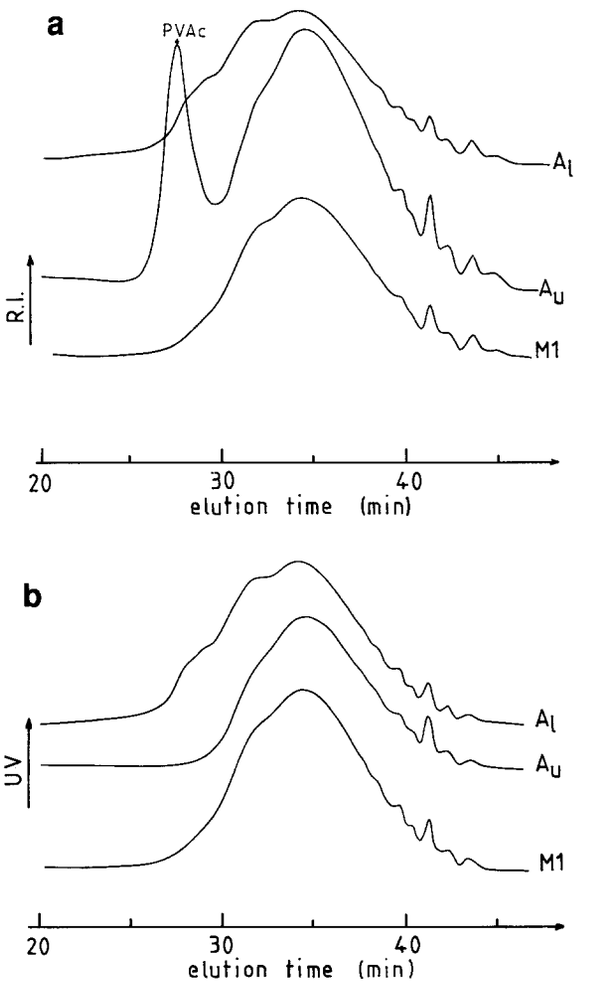

Figure 2 Gel permeation chromatograms for point A, A_u and A_l in *Figure 1*. (a) Recorded by an RI detector; (b) recorded by a u.v. detector at 254 nm

Table 2 Molecular weights of UP prepolymers in phases A, A_u and A_l of *Figure 1*

	M_n		M_w	
UP prepolymer in	RI[a]	u.v.[b]	RI[a]	u.v.[b]
Phase A	1689	1942	12630	11322
Phase A_u	–	1823	–	5693
Phase A_l	2005	1990	22475	34277

[a] Measured by a differential refractometer detector
[b] Measured by an ultraviolet detector

polydispersity (*Figure 2*, *Table 2*) and then causes the phase diagram to deviate from the CPC. This is why the points A_u, B_u, A_l and B_l are not located on the isothermal CPC in *Figure 1*. However, the CPC is more practical and useful for indicating the miscibility of the system than the deviating phase diagram. (From now on a phase diagram will refer to a miscibility diagram shown by the CPC instead of a real equilibrium phase diagram.)

The miscibility of the UP prepolymer with styrene monomer could be changed by changing the molecular characteristics of the UP prepolymer. *Figure 3* shows a comparison of the miscibility of the two prepolymers (M1 and M2) without LPA in the styrene by non-isothermal CPCs. The non-isothermal CPC is drawn from the cloud points (or cloud temperatures) observed by changing the mixture temperature at each composition. Under the CPC is a two-phase region and above the CPC is a one-phase region. The curves are similar to an upper critical solution temperature (UCST) curve for most of the binary polymer solutions[31]. To obtain a miscible resin, one needs either to increase the temperature or to increase the UP content. However, the former is not practical for storage and the latter would increase the resin viscosity which limits the introduction of fillers and fibres.

In *Figure 3* the M2 prepolymer is more miscible with styrene than the M1 prepolymer because the non-isothermal CPC of M2 is lower than that of M1. At room temperature the cloud point of M2 is ~72 wt% styrene, while that of M1 is ~60 wt% styrene. This implies that the M2 prepolymer has a higher percentage of styrene at room temperature and still remains in a one-phase region. The reason for this is believed to be due to the polydispersity and acid and hydroxyl indices of the prepolymers (*Table 1*).

The difference in miscibility of styrene between M1 and M2 also significantly influences the phase diagrams of the ternary (styrene–UP–LPA) system, shown in *Figure 1*, where the LPA is PVAc. The isothermal CPCs (at 23°C) of M1 and M2 are shown as the envelopes denoted by open and solid squares, respectively. In *Figure 3* M2 shows a smaller two-phase region than M1. One could conclude that a UP prepolymer which had better miscibility with styrene in a binary system will also show better miscibility with PVAc in the ternary system. Point C in *Figure 1* shows a formulation (13.3 wt% LPA, 41.3 wt% UP, 45.4 wt% styrene) used for later moulding and morphology studies. As shown in *Figure 1*, the formulation C with M1 is in the two-phase region, but with M2 is a miscible system.

In contrast to the isothermal ternary CPCs shown in *Figure 1*, *Figures 4* and *5* show non-isothermal ternary CPCs of prepolymers M1 and M2, respectively, with styrene and PVAc. The weight fraction of PVAc in the mixture of PVAc and UP prepolymer is x = (weight of PVAc)/(weight of PVAc + weight of UP prepolymer).

In *Figure 4*, the dashed, broken and solid lines represent the non-isothermal CPCs of M1 with styrene

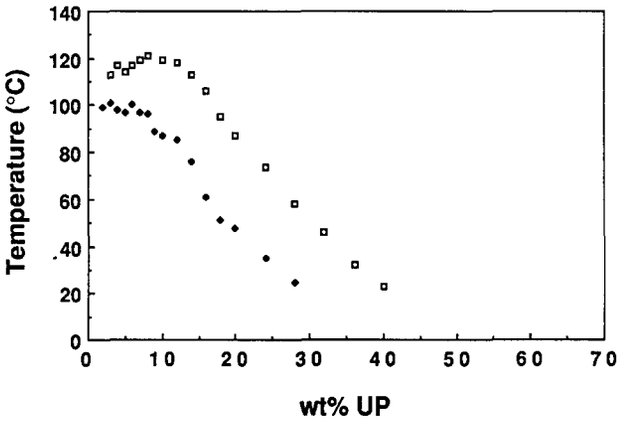

Figure 3 Non-isothermal CPCs for styrene–UP prepolymer binary systems. □, MI–styrene; ◆, M2–styrene

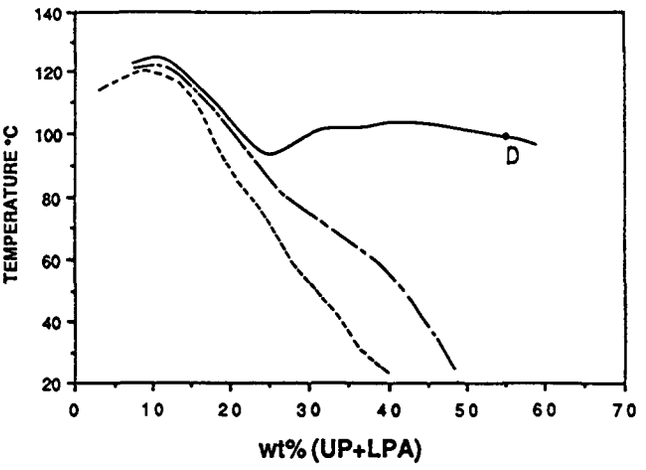

Figure 4 Non-isothermal CPCs for styrene–M1–PVAc ternary system: -----, $x=0$; – – –, $x=0.10$; ——, $x=0.25$, where x = (wt PVAc)/(wt PVAc + wt M1). Point D is the cloud temperature of a system with composition corresponding to point C in *Figure 1*

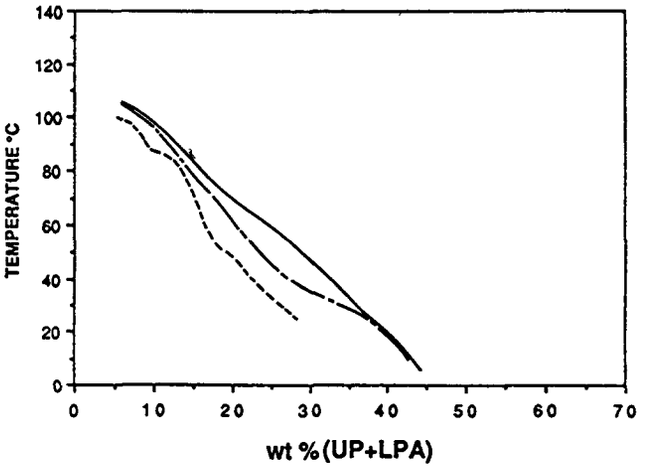

Figure 5 Non-isothermal CPCs for styrene–M2–PVAc ternary system: -----, $x=0$; – – –, $x=0.11$; ——, $x=0.25$, where x = (wt PVAc)/(wt PVAc + wt M2)

and PVAc with different PVAc contents ($x=0$, 0.1, 0.25, respectively). It is clearly shown that the addition of PVAc increases the cloud temperature of the system and makes the system more immiscible due to an enlarged two-phase region. Point D represents the cloud temperature (around 100°C) of a system with composition corresponding to point C in *Figure 1*. This means that the formulation C (13.3% PVAc, 41.3% M1, 45.4% styrene) will not be miscible until the temperature is >100°C. However, the cloud temperature for a similar system but with M2 is <0°C as can be seen in *Figure 5*. *Figure 5* shows the non-isothermal CPCs of M2 with styrene and PVAc at $x=0$, 0.11 and 0.25. Also, the addition of PVAc increases the cloud temperature and makes the system more immiscible. Nevertheless, the influence of PVAc on the system's miscibility with M2 is not significant as with M1.

Instead of PVAc, four PUs are used as LPA to mix with styrene and M1 prepolymer. They have similar molecular structures but have different molecular weights ranging from 2500 to 20000. The complete isothermal ternary CPCs are represented in *Figure 6*. They have a similar shape as the CPC in *Figure 1* but have smaller two-phase regions. The PU with the smallest molecular weight, i.e. PU2500, shows the smallest two-phase region. An increase in molecular weight results in an enlargement of the two-phase region, and then the corresponding CPC covers more of the industrial formulations shown in the dashed triangle region. This corresponds to a general trend used for polymer blends that a higher molecular weight polymer has a lower miscibility to form homogeneous polymer blends[31].

Phase separation and reaction kinetics

The polymerization of a ternary system (13.3 wt% PVAc, 41.3 wt% M2, 45.4 wt% styrene) was carried out in a differential scanning calorimeter and in a microscope hot-stage equipped with LALLS. The results are shown in *Figure 7*. Reaction conversions and exothermic rates are shown in *Figure 7* and are drawn as a function of reaction temperature. The reaction starts at ~100°C and ends at ~195°C and exhibits a maximum reaction rate at ~124°C.

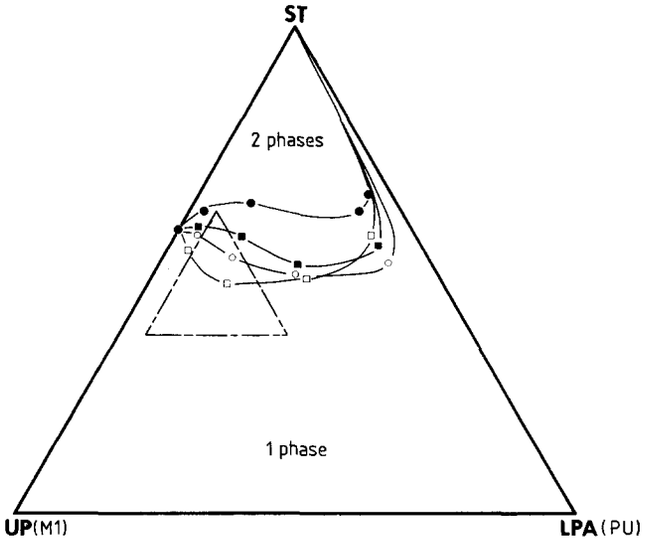

Figure 6 Isothermal CPCs for styrene–M1–PU ternary systems at 23°C. ●, PU2500; ■, PU9000, ○, PU11000, □, PU20000

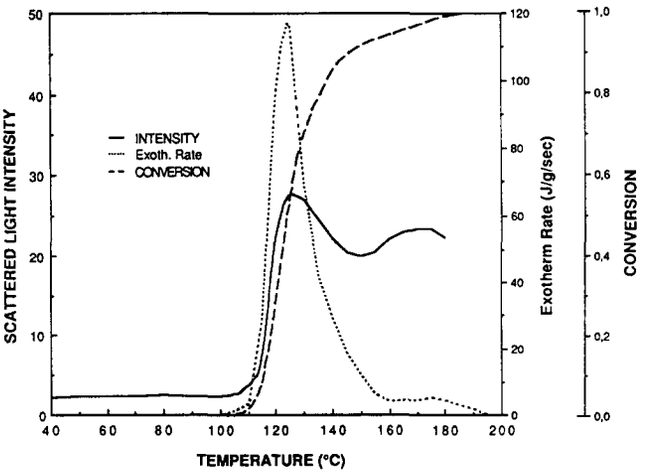

Figure 7 LALLS and d.s.c. results for a styrene–M2–PVAc ternary system reacted in a temperature scanning mode with a heating rate of 5°C min^{-1}. The scattered light is measured in an arbitrary unit

Figure 7 shows scattered light intensity with a higher intensity output representing a greater extent of immiscible microdomains (>100 nm). The initial value is above zero, which is believed to be caused by dust on the cover glasses. The measured intensity does not significantly change until the temperature reaches 105°C. Above 105°C, the intensity increases gradually and then rises rapidly above 112°C, which means a great increase in microdomain concentration and also indicates the phase separation between a major phase and the microdomains. At 124°C, the intensity output reaches a maximum and then decreases.

Several reacting samples studied in *Figure 7* were quenched in liquid nitrogen at 108, 115, 120, 122, 124 and 143°C. All the quenched samples were photographed on an optical microscope. Below 108°C the sample remains transparent and no microdomains could be observed on the optical microscope. The sample turns slightly white and opaque at 108°C (*Figure 8a*). The microdomains are probably still too small to be observed with an optical microscope. However, the increase of the LALLS intensity output above 105°C and the occurrence of slight opacity indicate the beginning of phase separation during the reaction, even though the corresponding conversion (α) is <1%. At 115°C, phase separation is clearly observed in the micrograph *Figure 8b*. The relatively dark points are due to transmission light refracted by the microdomains. The microdomains are believed to be highly crosslinked and high molecular weight polyester microparticles[22]. The corresponding conversion is only about 7%, but the intensity output becomes sharply increased beyond that point. At 120°C, the phase separation becomes clearer (*Figure 8c*). The conversion is about 28%. No voids or cracks are observed.

Figure 8d shows the micrographs for the sample at 122°C ($\alpha=36\%$). The white area shows the phase of unreacted resin–LPA mixture. The grey area is the reacted and separated microdomain. The dark areas represent microvoids[6,17] because the voids completely scatter the transmission light. The microvoids tend to link with one another and form dendritic fissures[23,24] called microcracks (*Figure 8e* at 124°C, $\alpha=49\%$). However, the fraction of the dark area cannot be correlated to the real volume fraction of the microcracks.

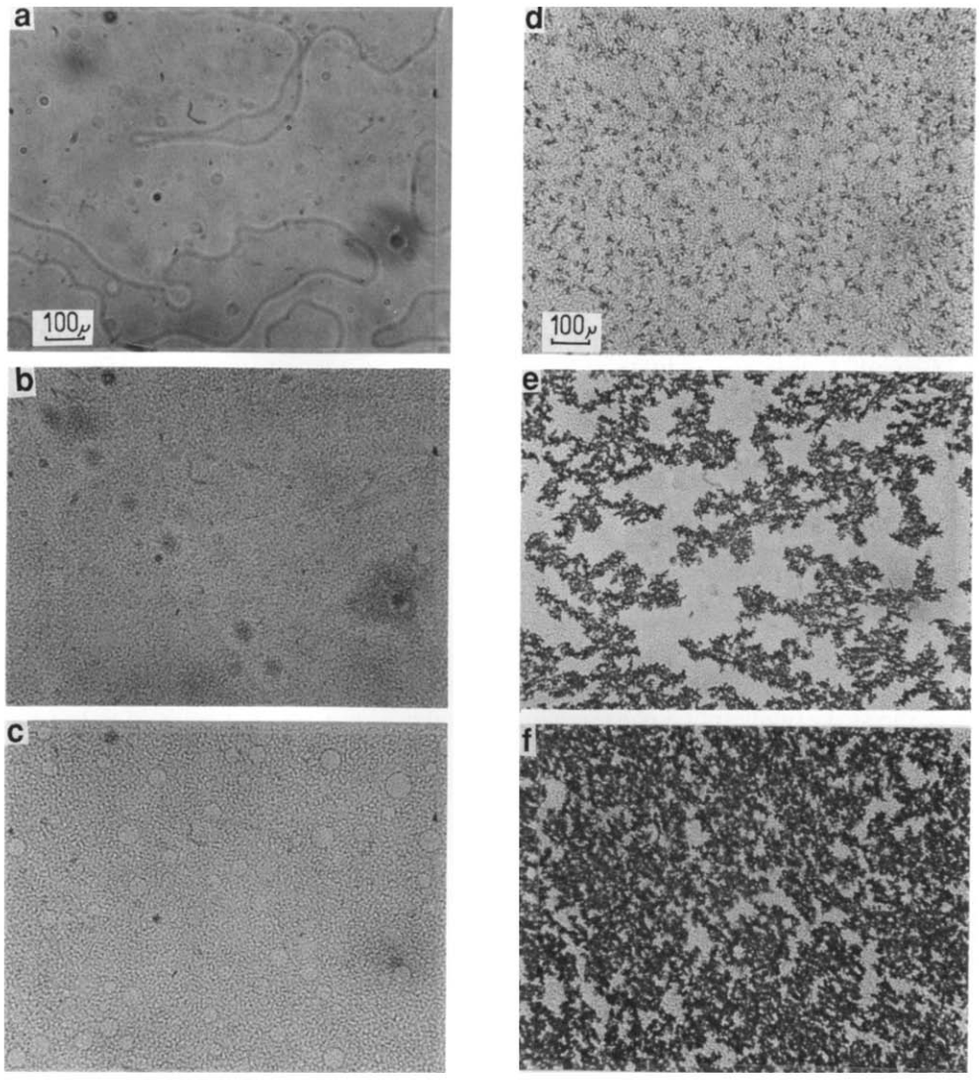

Figure 8 Optical micrographs of the quenched samples taken from LALLS scans in *Figure 8*: (a) at 108°C, $\alpha < 1\%$; (b) at 115°C, $\alpha = 7\%$; (c) at 120°C, $\alpha = 28\%$; (d) at 122°C, $\alpha = 36\%$; (e) at 124°C, $\alpha = 49\%$; (f) at 143°C, $\alpha = 88\%$. All micrographs have the same magnification

Usually, the dark area observed with the optical microscope is greatly overestimated because of serious light scattering by the voids. *Figure 8f* shows the micrograph for the sample quenched at 143°C. It reveals that microcracks exist throughout the sample near the end of the reaction ($\alpha = 88\%$). Due to strong light scattering the microcracks are overestimated by the dark areas.

Morphology

Ternary systems of 45.4 wt% styrene, 41.3 wt% UP and 13.3 wt% LPA were moulded. The morphology of the moulded samples was observed by scanning electron microscopy (SEM) and transmission electron microscopy (TEM). The SEM micrographs of the fracture surfaces of the systems styrene–M1–PVAc, styrene–M2–PVAc and styrene–M2–PU9000 after 30 min etching in acetone are shown in *Figures 9a–c*.

Figures 9a and *b* show typical fracture morphology of cured UP resins with PVAc[5,6,11]. The nodules shown are crosslinked polyester microparticles. These microparticles are also crosslinked with one another to form a continuous macronetwork which is insoluble in organic solvents. The PVAc is distributed around the microparticles and forms the other continuous phase. The PVAc phase on the fracture surface however, is washed out by etching in acetone for 30 min. In *Figure 9b* the size of the microparticle is singly distributed around 1–2 μm, while *Figure 9a* shows two size distributions of the nodules: one >10 μm and one <2 μm. The reason for this is due to the miscibility difference between M1 and M2.

Figure 9c shows the fracture morphology of the system styrene–M2–PU9000. The nodules cannot be individually observed. *Figure 9c* shows a more homogeneous morphology and is similar to a one-phase flake-like structure of a pure UP resin[32]. Nevertheless, the d.s.c. investigation reveals two glass transition temperatures at -35°C (PU phase) and 100°C (UP phase). This indicates that the cured resin is still a two-phase system. The extremely tiny particles composing the polymer network are coagulated and cannot be distingushed by SEM.

Figures 10a–d show the TEM micrographs of the moulded samples of UP resin (styrene–M2) with PVAc.

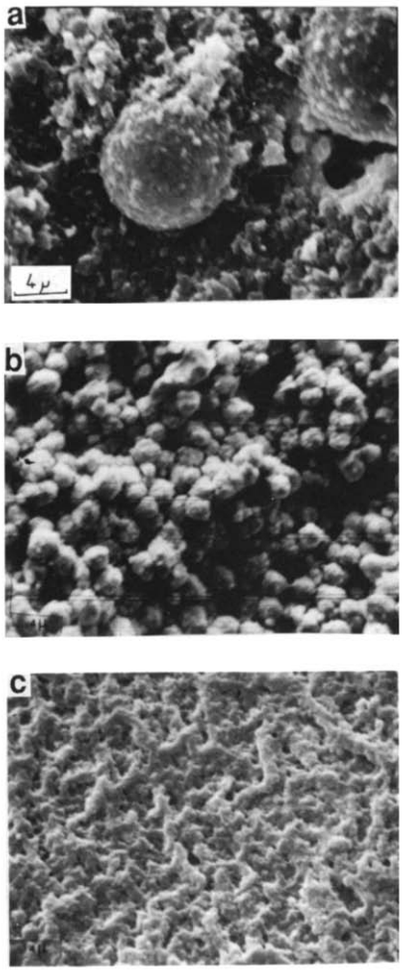

Figure 9 Scanning electron micrographs of moulded styrene–UP–LPA ternary systems: (a) styrene–M1–PVAc; (b) styrene–M2–PVAc; (c) styrene–UP–PU9000. All the micrographs have the same magnification

PU2500, PU9000 and PU20000, respectively. For a styrene–M2–PVAc system, *Figure 10a* shows a similar result to *Figure 9b* that the crosslinked UP phase exists as a form of nodules, shown as grey microparticles in *Figure 10a*, and forms a polymer network through linking the nodules. In contrast to *Figure 9b*, *Figure 10a* clearly shows the PVAc phase stained as the dark area. The PVAc phase exists around the polyester nodules and forms a second continuous phase. The white areas in the PVAc phase are the voids which are the so-called 'microvoids' which contribute to the shrinkage compensation for the UP resin[13–18,24].

Replacing PVAc with PU2500, the TEM micrograph reveals a nearly homogeneous morphology, as shown in *Figure 10b*. Although it does not show sharp contrast, one can still see a two-phase morphology: a grey area for the UP phase and a darker area for the PU phase. Nevertheless, the microvoids still exist and are shown as many tiny white points.

On increasing the molecular weight of PU from 2500 to 9000, one obtains the TEM micrograph shown in *Figure 10c*. Two-phase mophology exists: a PU phase (dark area) and a UP phase (grey area). The morphology is less homogeneous than that in *Figure 10b*. The microvoids can still be observed as white areas and are larger than those shown in *Figure 10b*. Because the PU phase is well distributed in the UP phase, when the PU phase is washed out by solvent, the UP phase would not show a nodular morphology like that in *Figure 9b*. This is why the SEM micrograph (*Figure 9c*) shows a rough surface morphology.

The inhomogeneity and size increase of microvoids are more enhanced for the system styrene–M2–PU20000 (*Figure 10d*). Again, the PU phase (dark area) is around the UP phase (grey area). The microvoids are larger and still exist in the LPA phase. This morphology is close to that shown in *Figure 10a* with PVAc.

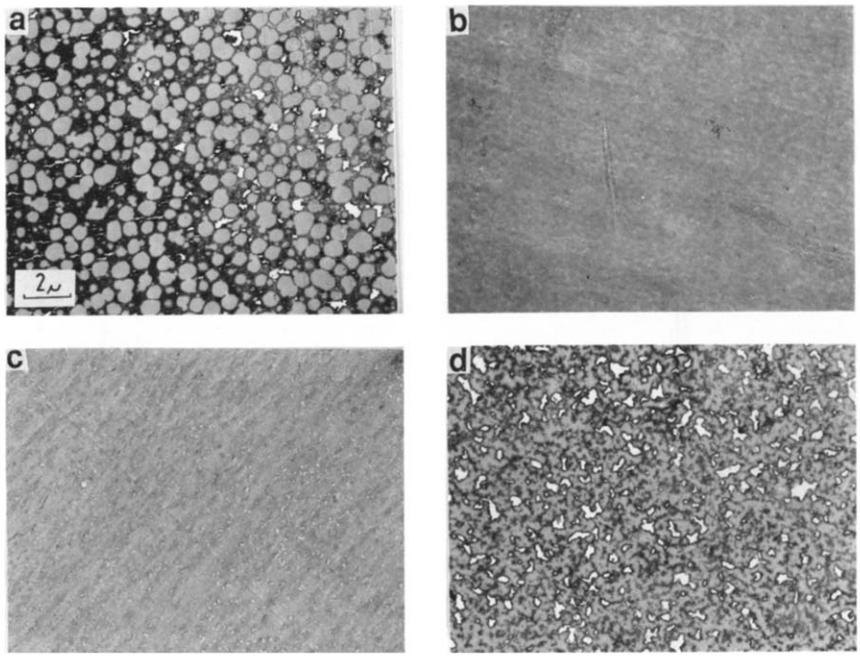

Figure 10 Transmission electron micrographs of moulded styrene–M2–LPA ternary systems: (a) PVAc; (b) PU2500; (c) PU9000; (d) PU20000. All the micrographs have the same magnification

Extract analysis

The moulded samples were also ground and extracted by DCM. The DCM extracts were first analysed by g.p.c. *Figure 11* shows g.p.c.–RI and g.p.c.–u.v. elution curves of the DCM extract of moulded styrene–M1–PVAc sample. The styrene peaks are not shown. The large left peak on the RI curve represents the PVAc extracted by DCM (cf. *Figure 2a*); it is not shown on the u.v. curve as there are no C=C groups.

The u.v. curve shows that some polymer molecules were not crosslinked in the moulded polymer network and were extracted by DCM. Similar results are also observed for other moulded samples. The g.p.c. however, cannot identify the extractable polymer molecules. A further composition analysis of the DCM extract was carried out by ^{1}H n.m.r.

Figure 12 shows ^{1}H n.m.r. results of the solid content in the DCM extract of moulded styrene (52.4 wt%)–M1 (47.6 wt%) sample without LPA. The spectrum clearly shows peaks for polystyrene[33]. This means that, during the curing, some styrene monomers tend to homopolymerize and form uncrosslinked and extractable polystyrene molecules. This is because at the final stage the styrene–styrene reaction is more favourable than the styrene–polyester and polyester–polyester reactions[32] due to the high immobility of polyester chains in the crosslinked network. *Figure 12* also shows proton peaks (around 1.2 ppm) of the CH_3 groups of propylene glycol[33]. This means that some polyester molecules remain in the DCM extract. However, the n.m.r. spectrum does not show any peak for the fumarate or maleate unsaturated bonds. This suggests that the peaks around 1.2 ppm belong to saturated polyester molecules which are formed during the synthesis of UP prepolymer due to the Ordelt effect[34,35].

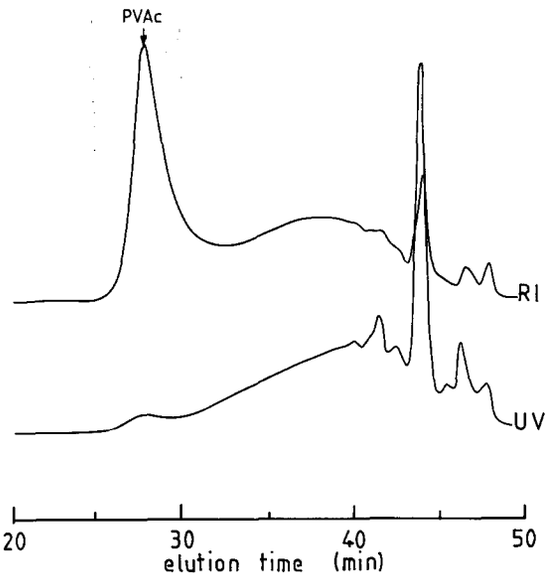

Figure 11 Gel permeation chromatography elution curves of the dichloromethane extract of moulded styrene–M1–PVAc using an RI detector and a u.v. detector

Figure 13 shows the ^{1}H n.m.r. spectrum of the solid content in the DCM extract of moulded styrene–M1–PVAc. Polystyrene peaks are seen in *Figure 13* indicating styrene homopolymerization occurs in the moulding of low profile UP resin. In addition, CH_3 peaks of saturated polyester are found in the n.m.r. spectrum. *Figure 13* also shows peaks belonging to PVAc[33]. Comparing *Figure 13* with *Figure 11*, one can conclude that the u.v. curve of *Figure 11* represents the free polystyrene molecules formed during the moulding.

Table 3 illustrates some results of the composition analyses of moulded UP resins with/without LPAs. For all the moulded samples, residual styrene monomer, saturated polyester and uncrosslinked polystyrene always exist in the DCM extract. A moulded styrene–M1 sample contains 2.1 wt% of residual styrene and 1.7 wt% of uncrosslinked polystyrene. The extracted LPA contents for all the moulded samples with LPAs are found to be less than the original amount of 13.3 wt%. This may be because some LPAs are trapped in the UP crosslinked network and cannot be extracted. The amount of uncrosslinked polystyrene is found to be higher (4–5 wt% of total amount or 5–6 wt% of neat resin) in the moulded samples with LPAs than in those without LPA. In other words, the addition of LPAs seems to enhance the styrene homopolymerization. The moulded styrene–M1–PVAc

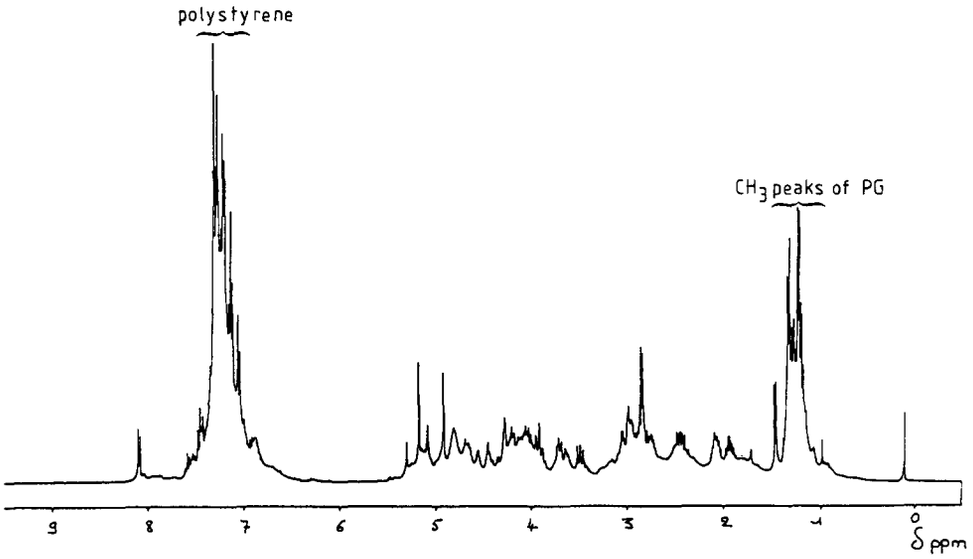

Figure 12 ^{1}H n.m.r. spectrum of solid content in the dichloromethane extract of moulded styrene (52.4 wt%)–M1(47.6 wt%) without LPA

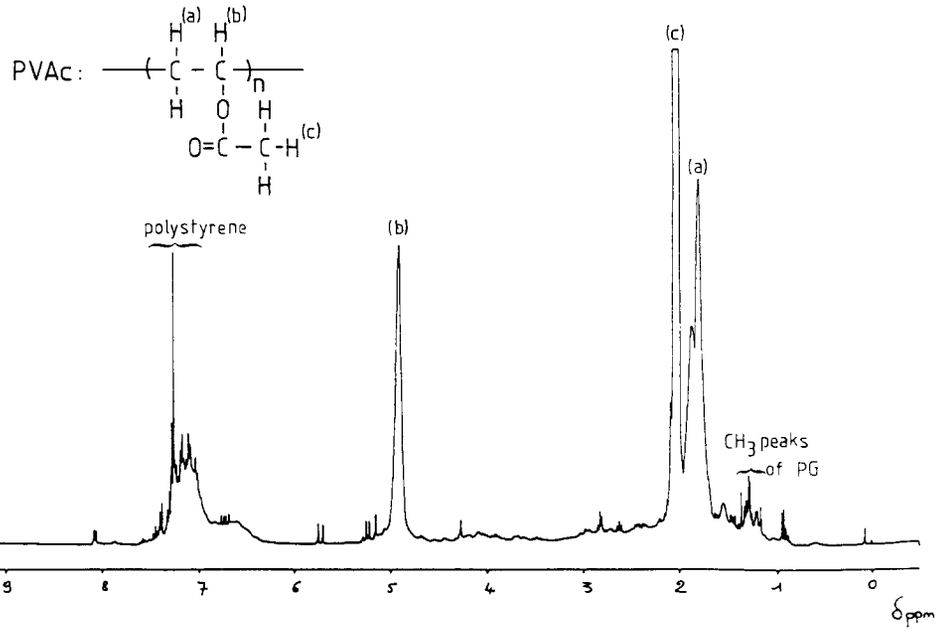

Figure 13 ^1H n.m.r. spectrum of solid content in the dichloromethane extract of moulded styrene (45.4 wt%)–M1(41.3 wt%)–PVAc(13.3 wt%)

Table 3 Composition analyses of dichloromethane extracts of moulded UP resins with/without LPAs

Compounds	Styrene–M1[a]	Styrene–M1–PVAc[b]	Styrene–M2–PVAc[b]	Styrene–M2–PU9000[b]
Styrene (%)	2.1 (2.1)	4.4[c] (5.1)[d]	1.8 (2.1)	5.2 (5.9)
Polystyrene (%)	1.7 (1.7)	4.1 (4.7)	4.5 (5.2)	5.1 (5.9)
LPA (%)	0.0	11.5	10.0	10.4
Saturated polyester (%)	1.2 (1.2)	1.0(1.2)	1.1 (1.3)	1.1 (1.3)

[a] Moulding composition: 52.4 wt% styrene, 47.6 wt% UP
[b] Moulding composition: 45.4 wt% styrene, 41.3 wt% UP, 13.3 wt% LPA
[c] Percentages based on the moulding compounds including LPA
[d] Percentages in parentheses based on the weight of neat resin, i.e. styrene and UP prepolymer only

sample shows a higher residual amount of styrene monomer than the styrene–M1 sample. However, the moulded styrene–M2–PVAc and styrene–M2–PU9000 samples show a similar residual amount of styrene as the styrene–M1 sample. The influence of the additional LPAs on the styrene residue is still not clear and needs to be studied further. The amount of saturated polyester remains constant for all the samples.

DISCUSSION

Relationship of phase diagram and morphology

For simplicity, a ternary phase diagram is used for a non-reactive system such as styrene–UP–LPA resin without initiators (*Figure 1*). The diagram shows the miscibility of the system before polymerization. During the reaction, due to polymer formation and decrease of monomer content, the phase diagram becomes dynamic and is too complicated to be obtained. However, a static phase diagram before reaction can be correlated to the morphology of the moulded resins.

In *Figure 1*, point C for a styrene–M1–PVAc system is located in a two-phase region but is in a one-phase region for the styrene–M2–PVAc system. The better miscibility of the M2 system is believed to be due to a narrower polydispersity and a lower acid index. From *Figure 9* it can be seen that the styrene–M2–PVAc system shows a more homogeneous nodule distribution than the styrene–M1–PVAc system. Moreover, the M2 system shows a better shrinkage compensation effect than the M1 system. This indicates that the system miscibility changed by prepolymer characteristics, shown on the ternary phase diagram, greatly influences the final product morphology.

In addition to prepolymer molecular effect, the LPA characteristics, such as molecular structure and molecular weight, also affect the ternary phase diagram and further affect the final morphology. *Figures 1* and *6* show the different phase diagrams of styrene–M1 resin mixing with PVAc and four PUs.

According to Van Krevelen[36], the solubility parameters of PVAc and PU used in this work are 9.3 and 9.2 $(cal/cm^3)^{1/2}$, respectively. The two types of LPAs have practically the same miscibility with styrene and UP prepolymer with respect to their similar solubility parameters. Therefore, if specific interactions such as hydrogen bonding are neglected, the miscibility of the UP resin with LPA seems to be only affected by the molecular weight of the LPA. *Figure 6* shows that increasing the molecular weight of LPA from 2500 to 20 000 gradually decreases the miscibility of the ternary system. It is also found that the CPC curve of PU20000

shows a crossover with those of PU9000 and PU20000. The reason for the crossover is due to a broader *MWD* of PU20000 than for the other PUs. In *Figure 1* the molecular weight of the PVAc is ~40 000 which is higher than the molecular weights of the PUs. This is probably why PVAc shows a less miscible phase diagram (*Figure 1*) than the PUs (*Figure 6*).

From *Figures 1* and *6* the miscibility order for the styrene–M1–LPA system using LPAs is PU2500 > PU9000 > PU11000 > PU20000 > PVAc according to the area change in the two-phase envelope. This order is also true for the system styrene–M2–LPA. For the moulding composition (i.e. point C in *Figure 1*) of the styrene–M2–LPA system, the mixture is always located in the miscible one-phase region at room temperature before reaction. After moulding, the SEM (*Figure 9*) and TEM results (*Figure 10*) reveal that the order to form a homogeneous morphology is still the same. For shrinkage compensation, the order is PU20000 > PU11000 > PU9000 > PU2500. The general trend is an increase of PU–LPA molecular weight may decrease the volume shrinkage of moulded UP resins[37]. PVAc however, does not show the best shrinkage compensation among the LPAs. Its effect is between PU11000 and PU9000. It implies that the molecular structure of the LPA may still play a role in shrinkage compensation.

All the results imply that a static phase diagram can be a good indicator for predicting the morphology and the shrinkage trend of the moulded parts. A low profile UP resin which has better storage miscibility can usually lead to a more homogeneous morphology and influences the curing shrinkage control. However, the experimental correlation between the phase diagram and the final morphology needs to be further studied.

Phase separation

According to phase equilibrium theory, a mixture which is located in the two-phase region of a phase diagram will eventually sediment into two distinct phases. The point A, for example, in *Figure 1*, forms an upper phase A_u and a lower phase A_l. The phase A_u is rich in styrene and PVAc, while phase A_l is rich in UP prepolymer. Nevertheless, the UP prepolymer is not homogeneously distributed in both phases because it is not a single molecular weight prepolymer but a prepolymer mixture with a broad *MWD*. *Figure 2* and *Table 2* reveal that the lower phase contains more high molecular weight prepolymers than the upper phase. These results indicate that, when phase separation takes place in the styrene–UP–LPA system, the high molecular weight prepolymer probably remains in the UP-rich minor phase, while the LPA remains in the styrene-rich major phase.

Adding an initiator and increasing the temperature starts the polymerization of the styrene–UP–LPA system. The polymerization of UP resin is a free radical chain-growth reaction. At the beginning of the reaction some high molecular weight polymer chains are formed by free radical growth. Due to the effect of intramolecular crosslinking reaction[38], the high molecular weight polymer chains immediately become highly intracrosslinked and extremely tiny particles. Those highly intracrosslinked, high molecular weight polymer particles are called 'microgels'[10,22,38]. These microgels may or may not be miscible in the system, depending on the dynamic phase diagram.

If one considers the microgel as a miscible high molecular weight UP molecule, the addition of microgel increases the polydispersity of the UP component and then will change the CPC on the phase diagram. For example, point C in *Figure 1* for styrene–M2–PVAc is initially located in the one-phase region. When the reaction takes place, the microgels are continuously formed. This means that the M2 polydispersity is dynamically increased. Consequently, the CPC envelope moves down and becomes larger. At a certain moment, the expanding CPC envelope may cover point C. This means the system becomes immiscible and will be phased out. When phase separation occurs, the LPA remains in the styrene-rich phase and the high molecular weight microgels are precipitated into the UP-rich phase. This is the 'fractionation' effect caused by LPAs.

Phase separation was clearly observed in *Figure 7*. The scattered light intensity starts to increase at ~108°C, where the conversion is <1%. Even at 115°C, although phase separation is significant, the conversion is only 7%. This indicates that phase separation occurs at the very beginning of the reaction when the microgel concentration is relatively low. Before phase separation, the microgel can be considered as an individual unit with no interference with another microgel.

When phase separation occurs, the microgels are precipitated into the UP-rich phase which is dispersed in the styrene-rich phase. In the UP-rich phase, the microgels are concentrated and then coagulate to form a larger particle which are called microparticles or nodules (*Figure 9*). The microparticle is composed of a number of microgels depending on the system and it is a basic crosslinking unit of the macronetwork.

As the reaction goes on, the styrene and the UP prepolymer in the styrene-rich phase continuously polymerize to form microgels which are then phased out and become microparticles. The microparticles are then crosslinked to form a macronetwork structure. Finally, only LPA is left in the styrene-rich phase when all the monomers have reacted. The LPA forms a second continuous phase which surrounds the polymer macronetwork. This morphology can be easily observed in *Figures 9b* and *10a*.

The system styrene–M1–PVAc shows a similar mechanism to that of styrene–M2–PVAc. In *Figure 1* point C is located in the two-phase region for styrene–M1–PVAc. Before the reaction, the system remains as two phases even at 100°C (shown as point D in *Figure 4*). When the reaction begins, the styrene-rich phase will follow the mechanism given for styrene–M2–PVAc. The microparticles formed in this phase show a similar size distribution as those in the system styrene–M2–PVAc (cf. *Figures 9a* and *b*). The UP-rich phase dispersed in the styrene-rich phase would also follow a similar mechanism. However, due to its low LPA content, the fractionation effect is not significant. Consequently, each dispersed UP-rich microdomain finally forms a large microparticle in the network structure. This morphology is observed in *Figure 9a* as the larger nodules.

When the PUs are applied, their greater miscibility changes the moment of phase separation and the final morphology. For example, PU2500 has the best miscibility and it shows the smallest CPC envelope on the phase diagram among the PUs and PVAc. This means that the styrene–UP–PU2500 system needs a longer time

to reach the point of phase separation. Consequently, the microgel concentration becomes large and the system turns to a gel near or before phase separation. The polymer macronetwork is then composed of tiny microgels. This is why the final morphology is homogeneous (*Figure 10b*). The mechanisms for PU9000, PU11000 and PU20000 and their morphology results are between those for PVAc and PU2500 (*Figure 10*).

Microvoid formation

Microvoid formation is believed to be a key role in shrinkage compensation for the UP resin[16,17,22–24]. *Figures 7* and *8* show that the microvoids are formed after phase separation near the maximum reaction rate. *Figure 10* clearly shows that the microvoids exist in the LPA phase but not in the interfacial area between the LPA and UP phases as mentioned previously[16,17,22–24]. These results indicate that phase separation is one of the necessary conditions to form microvoids.

After phase separation when the network is gradually constructed by the separated microparticles, near the maximum reaction rate the reaction takes place very fast and creates a strong shrinkage force or stress. The shrinkage stress then passes through the interfacial area into the LPA phase. Because the LPA is a weak thermoplastic, the shrinkage stress tears off the LPA phase and forms microvoids in the LPA phase (*Figure 8d*). Then the microvoids scatter the transmission light of LALLS, which significantly decreases the intensity output. In *Figure 7*, the decreasing light intensity beyond 124°C is due to microvoid formation and cannot be used for observing phase separation.

From *Figure 10*, one finds that a less homogeneous system has bigger microvoids and shows better shrinkage control. The microvoids only occur in the LPA phase. A less homogeneous system can leave a thicker LPA phase which allows formation of bigger microvoids. In contrast, the LPA phase in an homogeneous system is thinly distributed, so that it can only allow tiny microvoids in the phase (*Figures 10b* and *c*).

For a fast reaction, such as SMC moulding of pure resin without LPA, the shrinkage stress tears off the UP macronetwork and forms microcracks in the final products. The microcracks break the macronetwork and lead to a broken moulded part. Moulding with LPA, the microcracks are only located in the LPA phase and do not destroy the UP network. The LPA phase acts as a channel or a buffer area for microcrack propagation. Shrinkage stress cannot penetrate into fillers and fibre glasses. It finally forms microcracks around the fillers and fibre glasses[13], which also partly compensates for volume shrinkage.

LPA mechanism

It is well known that small amounts of thermoplastics in UP resin may cause low shrinkage or low profile behaviour. Although there are many explanations for the observed low profile phenomena[15], it is generally agreed that the formation of a two-phase structure is a major factor for shrinkage compensation. Combining all the results, one may formulate a general low profile mechanism. A schematic drawing is shown in *Figure 14*. The deviation from the general mechanism caused by the characteristics of prepolymers and LPAs will be discussed later.

First step – storage stage. At room temperature, during storage or before reaction, the low profile resin may be a one-phase system (e.g. styrene–M2–PVAc) or may be a dispersed two-phase system (e.g. styrene–M1–PVAc). For the dispersed two-phase system, phase A represents a styrene-rich phase and phase B represents a UP-rich phase (cf. *Figure 11*). Phase A is a continuous phase while phase B is dispersed in phase A.

Second step – heating stage. During moulding, the resin is first heated from the storage temperature to the moulding temperature. The increasing temperature improves the miscibility of the system. When the temperature is higher than the corresponding cloud temperature, the system becomes miscible and transparent.

Third step – phase separation stage. When the reaction takes place, highly crosslinked, high molecular weight microgels are formed. This decreases the miscibility of the overall reacting system. As the blend reaches a corresponding dynamic cloud point, phase separation occurs. Consequently, the microgels are phased out in a dispersed phase and then form microparticles which become the units of the following macronetwork structure. The continuous phase is a styrene-rich phase. In this stage, the scattered light intensity measured by LALLS starts to increase.

Fourth step – macrogelation stage. When the microgel or microparticle concentration reaches a certain point, a macronetwork structure begins to be set up through the crosslinkings of the microparticles or microgels. The macronetwork structure may grow and become stronger as the reaction goes on. This macrogelation stage may be

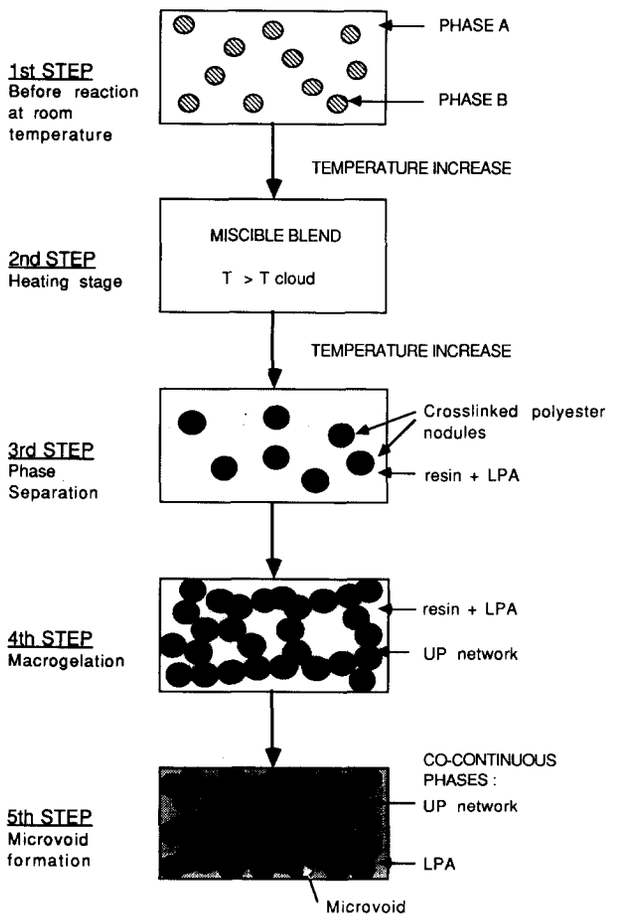

Figure 14 Proposed LPA mechanism for the curing of UP resins

before or after the phase separation stage. After this point, the system contains two continuous phases. The styrene-rich phase gradually becomes a LPA-rich phase due to consumption of the reactants.

Fifth step – microvoid formation stage. As the reaction goes to near the maximum rate point, the fast reaction creates strong shrinkage stress in the UP phases. The stress passes through the interfacial region into the LPA phase and then creates microvoids in the LPA phase. The microvoids formed eliminate the shrinkage stress and compensate partly for the volume change due to resin shrinkage. At this stage, the measured light intensity by LALLS starts to decrease due to strong light scattering by the voids and becomes meaningless.

The LPA mechanism mentioned above is general. The characteristics of UP prepolymers and LPAs may cause some deviation from the general path. For example, a system such as styrene–M2–PVAc will miss out the first step because of its good miscibility at room temperature. For styrene–M2–PU2500, the system becomes cloudy after the gel point. It seems that the third step comes after the fourth step. However, it is difficult to decide the order of the phase separation and the gelation point because the microparticles formed are too tiny to be detected by transmission light. For a system such as styrene–M1–PVAc, the second step does not exist. Phase B in the first step becomes a phase of crosslinked polyester nodules in the third step.

For a system containing PMMA, PS or PE as a LPA, the mechanism is quite different. These LPAs are highly immiscible in the UP resin. These low profile resins are always located in a two-phase region even at high moulding temperature. In contrast to the styrene–M1–PVAc system, the continuous phase, i.e. phase A in the first step, is a UP-rich phase, in which LPA (e.g. PMMA) is excluded. The dispersed phase, phase B, is a LPA-rich phase containing styrene, UP prepolymer and LPA. During the reaction, phase A follows a reaction mechanism of pure UP resin and then forms a flake-type fracture morphology[22,32]. Phase B, on the other hand, follows the mechanism of the system styrene–M2–PVAc. Consequently, it forms a nodule network, similar to that shown in *Figure 9b*, which is dispersed in a continuous bulk UP phase formed by phase A[13–18,22–24]. The microvoids only exist in the LPA phase of phase B. This is probably why PMMA shows a less significant effect on volume compensation than PVAc.

CONCLUSIONS

In this work, the morphology of a moulded low profile UP resin has been correlated with its static miscibility phase diagram before reaction. The correlation is further interpreted by phase separation taking place during reaction. A novel low profile mechanism has been proposed based on phase diagram results, phase separation phenomena and product morphologies. A phase separation is a necessary condition to form microvoids in the LPA phase. The proposed mechanism is a qualitative concept rather than a quantitative model. The real morphology formation during reaction is dependent on the reaction kinetics and phase separation. This will be greatly influenced by the process involved and the processing conditions, such as temperature and pressure. In adddition, although the microvoids are observed for volume compensation, the correlation of microvoid formation to volume control and surface quality of a moulded resin is still to be further investigated.

ACKNOWLEDGEMENTS

The authors gratefully acknowledge Dr H. Strub, Mr D. Nocq and Mr J. C. Jannel for their technical assistance. The support and permission to publish from CRAY VALLEY-TOTAL Group are also acknowledged.

REFERENCES

1 Horie, K., Mita, I., Kambe, H. *J. Polym. Sci. A1* 1970, **8**, 2839
2 Kubota, H. *J. Appl. Polym. Sci.* 1975, **19**, 2279
3 Kamal, M. R., Sourour, S. and Ryan, M. *SPE ANTEC Tech. Papers* 1973, **19**, 187
4 Lee, L. J. *Polym. Eng. Sci.* 1981, **21**, 483
5 Stevenson, J. F. *Polym. Proc. Eng.* 1983, **1**, 201
6 Han, C. D. and Lem, C. W. *J. Appl. Polym. Sci.* 1983, **28**, 3155, 3185, 3207
7 Kuo, J. F., Chen, C. Y., Chen, C. W. and Pan, T. C. *Polym. Eng. Sci.* 1984, **24**, 22
8 Yang, Y. S. and Lee, L. J. *J. Appl. Polym. Sci.* 1988, **36**, 1325
9 Yang, Y. S., Lee, L. J., Tom, S. K. and Menardi, P. C. *J. Appl. Polym. Sci.* 1989, **37**, 2313
10 Yang, Y. S. and Lee, L. J. *Polym. Process Eng.* 1988, **5**, 327
11 Silva-Nieto, R. J., Fisher, B. C. and Birley, A. W. *Polym. Eng. Sci.* 1981, **21**, 499
12 Marker, L. and Ford, B. *32nd SPI Tech. Papers* 1977, 16E
13 Bartkus, E. J. and Kroekel, C. H. *Appl. Polym. Symp.* 1970, **13**, 113
14 Kroekel, C. H. Paper presented at SEA Automotive Engineering Congress, Detroit, MI, January 1968
15 Atkins, K. E. 'Polymer Blends' (Eds. D. R. Paul and S. Newman), Academic Press, New York, 1978, Ch. 2, 391
16 Pattison, V. A., Hindersinn, R. R. and Shwartz, W. T. *J. Appl. Polym. Sci.* 1974, **18**, 2763
17 Pattison, V. A., Hindersinn, R. R. and Shwartz, W. T. *J. Appl. Polym. Sci.* 1975, **19**, 3045
18 Bucknall, C. B., Davies, P. and Partridge, I. K. *Polymer* 1985, **26**, 109
19 Lem, K. W. and Han, C. D. *Polym. Eng. Sci.* 1984, **24**(3), 175
20 Lee, D. S. and Han, C. D. *Polym. Comp.* 1987, **8**(3), 133
21 Lee, D. S. and Han, C. D. *Polym. Eng. Sci.* 1987, **27**(13), 964
22 Kiaee, L., Yang, Y. S. and Lee, L. J. *AIChE Symp.* 1988, **84**, 52
23 Ross, L. R., Hardebeck, S. P. and Backman, M. A. 43rd Ann. Conf., Comp. Inst., SPI Inc., 1988, 17C
24 Tomasana, M., Hidehiko, S., Kiyoshi, H. and Gwilym, E. O. 44th Ann. Conf., Comp. Inst., SPI Inc, 1989, 12F
25 Hsu, C. P. and Lee, L. J. *SPE ANTEC Tech. Papers* 1989, **35**, 598
26 Suspène, L. and Pascault, J. P. *J. Appl. Polym. Sci.* 1990, **41**, 2665
27 Suspène, L. and Pascault, J. P. *SPE ANTEC Tech. Papers* 1989, **35**, 604
28 Rosso, J. C., Guieu, R. and Carbonnel, L. *Bull. Soc. Chim.* 1970, **489**, 2849
29 Rosso, J. C., Guieu, R. and Carbonnel, L. *Bull. Soc. Chim.* 1970, **490**, 2855
30 Koningsveld, R. and Staverman, A. J. *J. Polym. Sci. A2* 1968, **6**, 349
31 Flory, P. J. 'Principles of Polymer Chemistry', Cornell University Press, Ithaca, 1953
32 Yang, Y. S. and Lee, L. J. *Polymer* 1988, **29**, 1793
33 Bovey, F. A. 'High Resolution NMR of Macromolecules', Academic Press, New York, 1972
34 Judas, D., Fradet, A. and Marechal, E. *Makromol. Chem.* 1984, **185**, 2583
35 Paci, M., Crescenzi, V. and Supino, N. *Makromol. Chem.* 1982, **183**, 377
36 Van Krevelen, D. W. and Hoftyser, P. J. 'Properties of Polymers– Correlations with Chemical Structure', Elsevier, Amsterdam, 1972
37 Melby, E. G. and Castro, J. M. in 'Materials and Processing in Comprehensive Polymer Science, Vol. 7: Specialty Polymers and Polymer Processing' (Ed. S. L. Aggarwal), Pergamon Press, New York, 1989
38 Dusek, K., Galina, H. and Mikes, J. *Polym. Bull.* 1980, **3**, 19